AN ANALYTICAL CHARACTERIZATION OF INITIALLY NON-HOMOGENEOUS MATCHED BEAMS AT EQUILIBRIUM*

R. P. Nunes#, CTI, FURG, Rua Eng. Alfredo Huch 475, CEP: 96201-900, Rio Grande, RS, Brasil
F. B. Rizzato†, IF, UFRGS, Av. Bento Gonçalves 9500, C.P. 15051, Porto Alegre, RS, Brasil

Abstract

Non-homogeneity is a characteristic naturally present in non-neutral beams. Recently, a set of works has been developed by us for the case of beams initially homogeneous, making possible that relevant macroscopic quantities such as the RMS radius and emittance could be determined at equilibrium as functions of characteristic parameters of beam phase-space and of initial conditions. The present work intends to investigate the influences of the initial inhomogeneity in the beam route to equilibrium. Through the same methodology introduced in the studies for the homogeneous beams, both emittance and beam envelope have been obtained as functions of the magnitude of the inhomogeneity and some additional parameters associated with geometry of beam phase-space. The results obtained with this investigation have proven to be useful not only to better understand the effects of inhomogeneity over beam dynamics but also to provide physical background to the investigations previously carried out for homogeneous beams.

INTRODUCTION

Homogeneous beams with mismatched envelopes usually evolve to an equilibrium-like state after some characteristic time during its magnetic focusing inside the confinement channel. This process is macroscopically characterized by a not negligible growth of emittance [1], which is a statistically-averaged beam quantity that involves spatial and velocity coordinates of its constituent particles. If beam is initially cold (all beam particles have velocities that can be neglected), one can assure that the increasing of emittance is unconditionally associated with increasing of particle velocities. Beam earns kinetic energy or, using jargons of the field, beam is progressively heated during magnetic focusing. Since overall energy is a constraint of beam motion, thus if kinetic energy increases (in this case from an initial zero value to some of equilibrium), effective potential energy must decrease, conserving total energy. Large non-linear resonances are responsible in to excite beam particles individually, converting potential energy stored in envelope oscillations into kinetic energy that supplies the chaotic movement of these particles [2][3].

Some similar emittance growth also occurs for initially non-homogeneous beams. Initially cold and inhomogeneous beams also direct to its equilibrium with a systematic heating of its particles [4]. Inhomogeneity leads beam fluid elements to oscillate with a frequency that is dependant of spatial position. Note the force that beam exerts over each particle is nonlinear, because its density is intrinsically non-homogeneous. Even consecutive fluid elements (those displaced initially with an infinitesimal spatial distance, that has in this way much similar oscillating frequencies), in a finite time will lose coherence and inevitably will collapse. From beam phase-space picture, this collapse will look like as particle jets, which are the forerunner instability for beam reaches its equilibrium. If envelope mismatch is eventually present, the previous commented large resonant islands also exist to provide kinetic energy to the particles of non-homogeneous beams. However, even in the absence o envelope mismatch, heating process still occurs, inducing phase-space mixing and consequently that beam reaches its equilibrium. This is due to another physical mechanism, which it has been called of charge redistribution by us. In the same manner particles couple with envelope oscillations, particles can also couple with charge redistribution oscillations. The main difference between both couplings is that the first one is resonant but the second one usually is not [3]. Resonant interaction is achieved in just some limit situations. But this discussion is out of scope of the current work.

The purpose of this work is to determine equilibrium quantities of an initially inhomogeneous beam as a function of its initial conditions. The system considered here is an initially cold, azimuthally symmetric, and non-homogeneous beam, focused by a constant magnetic field and encapsulated by a conducting pipe. Azimuthal symmetry has beam considered, which means that essentially initial state is represented by just the magnitude of inhomogeneity, here denoted as η. Beam is initially considered matched, situation in which envelope oscillations are negligible.

ANALYTICAL DESCRIPTION

One way of achieving the goal is to extend the methodology previously introduced in reference [5] for homogeneous beams to the case of an initially inhomogeneous beam. Here, beam has been considered inhomogeneous with a particle density $n_b(R, s=0)$ in a parabolic shape

$$n_b(R,s) = \begin{cases} \dfrac{N_b}{\pi r_{bo}^2} + \eta \dfrac{N_b}{\pi r_{bo}^2}\left(\dfrac{2R^2}{r_{bo}^2} - 1\right), 0 \le R \le r_{bo} \\ 0, r_{bo} < R \le r_w \end{cases} \quad (1)$$

in which r_{bo} represents beam envelope, R is the radial coordinate in the Larmor frame and r_w is the pipe radius. Quantity η designates the magnitude of inhomogeneity ascribed to the beam. Figure 1a shows the appearance of this density in phase-space for $\eta = 0.5$. All results have been computed by the means of full self-consistent N-

*CNPq and FAPERGS, Brazil.
#rogerpn@if.ufrgs.br, †rizzato@if.ufrgs.br

particle beam numerical simulations employing Gauss' Law to describe interactions between beam particles [3].

Particle density of equation (1) after some characteristic time τ (time in which halo is formed) assumes another format, which has to be modeled. A snapshot of beam phase-space at equilibrium is shown in Figure 1b. Note the absence of the curve region naturally present in the analysis of a homogeneous beam [2][3]. This is just because beam has been considered initially matched, which means $r_{bo} = 1$, with the same rescaling technique (of spatial and temporal variables) adopted for homogeneous beams [3][5]. Then halo in this case is composed by the warm particles, since hot particles do not exist. Beam density at equilibrium can be modeled as

$$n_b(R, s \geq \tau) = \begin{cases} n_c(R) + n_m(R), & 0 \leq R \leq r_c \\ n_m(R), & r_c < R \leq r_m \\ 0, & r_m < R \leq r_w \end{cases} \quad (2)$$

in which n_c is the core density and n_m is the halo density, composed by just the warm particles. Once particle jets expel all particles that makes n_b to be inhomogeneous, at $s \geq \tau$ n_c can be described by a homogeneous density

$$n_c(R, s \geq \tau) = (1 - f)N_b/\pi r_c^2, \quad (3)$$

in the same form it was in reference [2], in which r_c is core radius at equilibrium, f is the fraction of halo particles given by $f \equiv N_m/N_b$, and $N_c = (1 - f)N_b$ is the number of core particles since relation $N_b = N_c + N_m$ holds for every time of beam dynamics.

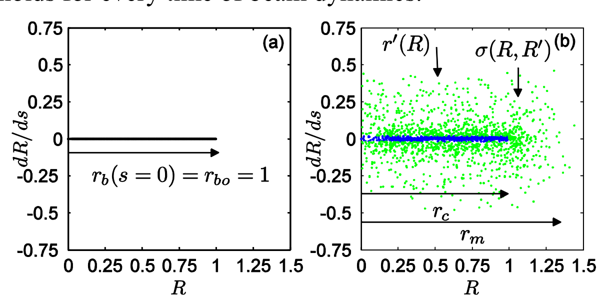

Figure 1: Beam phase-space structure in two distinct times of its dynamics inside the magnetic focusing channel. Panel (a) show beam phase-space at initial state $s = 0$ and (b) show beam phase-space after equilibrium is reached, at $s = 796.3$. Results have been obtained through numerical simulation with magnitude of inhomogeneity $\eta = 0.5$ and with a matched envelope of $r_b(s = 0) = r_{bo} = 1$.

The rectangular region where warm particles reside have to be also described. By visual inspection of Figure 1b, one can consider that particle density in phase-space is constant $\sigma(R, R') = \sigma$, which extends over horizontal axis by $0 < R < r_m$ and over vertical axis by $-r'(R) < R' < r'(R)$. In this case, $r'(R)$ is just a horizontal line, whose value is not important for the calculations. Considering this geometry aspects, density n_m assumes

$$n_m(R, s \geq \tau) = \frac{1}{\pi R}\int_0^{r'(R)} \sigma(R, R')dR = \frac{f N_b}{2\pi r_m}\frac{1}{R'}, \quad (4)$$

where r_m is the rectangular region size over R axis. Expression $N_m = \int d\theta dR R n_m$ for the number of warm particles has been employed to eliminate σ and other quantities of equation (4).

One should note that with equations (3) and (4), beam density at equilibrium $n_b(R, s \geq \tau)$ of equation (2) is completely defined. Note that equation (2) is dependant of fraction f, core size r_c, halo size r_m, and the total number of beam particles N_b. In fact, as one will notice in the next paragraphs, N_b is not a variable, because quantities of interest are per beam particles. Also, r_c and r_m are geometric parameters of beam phase-space, determinable *a priori* by visual inspection of simulation results. Actually, the only one free parameter in the model to be present will be the fraction of halo particle f. For the initial state, described by equation (1), the same reasoning holds. No variables exist, since beam is matched and η is a quantity defined as initial condition. Similar results have been obtained in reference [3] for homogeneous beams, being the main difference associated to the initial state, in which beam initial mismatch is replaced by the magnitude of inhomogeneity η.

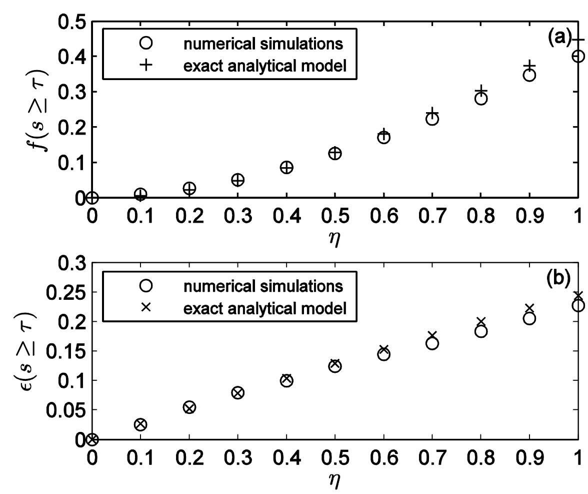

Figure 2: Comparison between results provided by numerical simulations and the exact analytical model as a function of magnitude of inhomogeneity η. Results are shown in (a) for the fraction f and in (b) for emittance ϵ.

Now it is the necessary moment of invoking energy conservation. Beam total energy is a constant of the motion. That is, once a given energy is initially ascribed to the system, it is possible to write an equation in the form

$$\frac{1}{2}\langle \mathbf{V}^2\rangle(s) + \frac{1}{2}\kappa_{zo}\langle \mathbf{R}^2\rangle(s) + \mathcal{E}_F(s) = E, \quad (5)$$

that relates beam energy stored by the particles (the first two terms, potential plus kinetic energy) and fields (last term, $\mathcal{E}_F(s)$), which is valid for the entire beam dynamics. Energy stored in the fields is given by

$$\mathcal{E}_F(s) = \frac{1}{4\pi K_b}\int |\nabla\psi|^2 d\mathbf{R}, \quad (6)$$

where dimensionless potential ψ satisfies

$$\nabla^2\psi = -\frac{2\pi K_b}{N_b} n_b(\mathbf{R}, s), \quad (7)$$

the Poisson Equation, for every time s. Beam perveance K_b and the coefficient of constant magnetic focusing κ_{zo} are unimportant due to rescaling scheme adopted [2].

In this way, one can compute energy at initial nonstationary state and energy at the final stationary state. Since energy is conserved, both obtained expressions can be equalized as

$$E(s=0) = E(s \geq \tau) = E = \text{constant}. \quad (8)$$

Energy at initial state $E(s=0)$ is evaluated inserting equation (1) into equation (5), with the aid of equations (6) and (7). The obtained expression has to be a function of just η. Energy at equilibrium $E(s \geq \tau)$ is determined in a similar fashion. Employing equation (8) to connect energy in both states and collecting terms in powers of fraction o halo particles f, one has a simple polynomial

$$D(r_c, r_m)f^2 + E(r_c, r_m)f + F(r_c, \eta) = 0, \quad (9)$$

in which the coefficients have the form

$$\begin{aligned} D(r_c, r_m) &= \frac{1}{2}\ln\left(\frac{r_m}{r_c}\right) + \frac{2r_c}{3r_m} - \frac{5}{8} \\ E(r_c, r_m) &= \ln\left(\frac{r_c}{r_m}\right) - \frac{2r_c}{3r_m} - \frac{r_c^2}{2} + \frac{r_m^2}{3} + \frac{3}{4}, \quad (10) \\ F(r_c, \eta) &= -\frac{1}{2}\ln(r_c) + \frac{r_c^2}{2} - \frac{\eta^2}{48} - \frac{1}{2} \end{aligned}$$

which are functions of just known quantities.

RESULTS

The results calculated for the fraction of halo particles f and for emittance ϵ at equilibrium through numerical simulations and the exact analytical model are compared in Figure 2. Satisfactory accordance between both is perceived. Calculations have been performed for many values of magnitude of inhomogeneity η, to say $0 \leq \eta \leq 1$, with steps of $\Delta\eta = 0.1$. For obviously aspects, beam envelope at equilibrium has not been calculated.

In Figure 3, a comparison between the core density n_c and the halo density n_h is done. Results provided by numerical simulations are represented with histograms and the ones provided by the exact analytical model appear as solid lines. Again, a nice agreement is obtained.

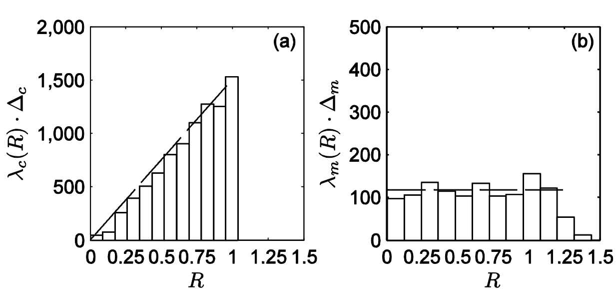

Figure 3: Histograms for beam particle density computed through numerical simulations (bins) and the exact analytical model (solid line). Comparison occur in panel (a) for beam core with $\Delta_c \cong 0.0866$ and in panel (b) for beam halo $\Delta_m \cong 0.1194$. Magnitude of inhomogeneity $\eta = 0.5$.

Finally, complete results about the comparison of the model with numerical simulations are shown in Table 1. There, for each η, the coefficients of polynomial in equation (9) are presented as well as results for beam equilibrium quantities of interest are shown. Further discussions will be a subject of future works.

Table 1: Comparison of the exact analytical model with results provided by numerical simulations for many values of magnitude of initial beam inhomogeneity η.

		$\eta = 0$	$\eta = 0.2$	$\eta = 0.4$
	r_c	$= 1$	$= 1$	$= 1$
	r_m	$= 1$	$\cong 1.3$	$\cong 1.3$
Exact analytical solution	$D(r_c, r_m)$	$= 1/24$	$\cong 0.019002$	$\cong 0.019002$
Exact analytical solution	$E(r_c, r_m)$	$= -1/12$	$\cong 0.038148$	$\cong 0.019002$
Exact analytical solution	$F(r_c, \eta)$	$= 0$	$\cong -0.000833$	$\cong -0.003333$
Exact analytical solution	f	$= 0$	$\cong 0.02161$	$\cong 0.08387$
Exact analytical solution	R_b	$= 1/\sqrt{2}$	$\cong 0.70807$	$\cong 0.71085$
Exact analytical solution	ϵ	$= 0$	$\cong 0.05239$	$\cong 0.10361$
Numerical simulation	f	$= 0$	$\cong 0.02630$	$\cong 0.08490$
Numerical simulation	R_b	$= 1/\sqrt{2}$	$\cong 0.71283$	$\cong 0.73364$
Numerical simulation	ϵ	$= 0$	$\cong 0.05475$	$\cong 0.09961$
		$\eta = 0,6$	$\eta = 0.8$	$\eta = 1.0$
	r_c	$= 1$	$= 1$	$= 1$
	r_m	$\cong 1.3$	$\cong 1.3$	$\cong 1.3$
Exact analytical solution	$D(r_c, r_m)$	$\cong 0.018919$	$\cong 0.019002$	$\cong 0.019002$
Exact analytical solution	$E(r_c, r_m)$	$\cong 0.043100$	$\cong 0.038148$	$\cong 0.038148$
Exact analytical solution	$F(r_c, \eta)$	$\cong -0.007500$	$\cong -0.013333$	$= -1/48$
Exact analytical solution	f	$\cong 0.18039$	$\cong 0.30359$	$\cong 0.44671$
Exact analytical solution	R_b	$\cong 0.71513$	$\cong 0.72057$	$\cong 0.72683$
Exact analytical solution	ϵ	$\cong 0.15287$	$\cong 0.19983$	$\cong 0.24450$
Numerical simulation	f	$\cong 0.17010$	$\cong 0.28090$	$\cong 0.40110$
Numerical simulation	R_b	$\cong 0.76578$	$\cong 0.79441$	$\cong 0.81434$
Numerical simulation	ϵ	$\cong 0.14447$	$\cong 0.18314$	$\cong 0.22734$

ACKNOWLEDGMENTS

This scientific research has been done with the aid of the National Centre of Supercomputation of the Brazil's South Region (CESUP), located at the Federal University of Rio Grande do Sul (UFRGS).

REFERENCES

[1] A. Cuchetti, M. Reiser, and T. Wangler, in Proceedings of the Invited Papers, 14th Particle Accelerator Conference, San Francisco, California (IEEE, New York, 1991), pp. 251.
[2] R. P. Nunes, R. Pakter, and F. B. Rizzato, J. Appl. Phys. 104, 013302 (2008).
[3] R. P. Nunes. PhD Thesis. UFRGS (2008).
[4] R. P. Nunes, R. Pakter, F. B. Rizzato, A. Endler, E. G. Souza, Phys. Plasmas 16, 033107 (2009).
[5] R. P. Nunes, and F. B. Rizzato, in Proceedings of the 2008 European Particle Accelerator Conference, Genoa, Italy. (EPS-AG, Genoa, 2008), pp. 3206.